ARCHIVES OF BIOCHEMISTRY AND BIOPHYSICS
Vol. 311, No. 1, May 15, pp. 13–18, 1994

DNA Strand Breaks Following *in Vitro* Exposure to Asbestos Increase with Surface-Complexed [Fe^{3+}]

Andrew J. Ghio,*,[1] Thomas P. Kennedy,* Jacqueline G. Stonehuerner,†
Alvin L. Crumbliss,† and John R. Hoidal‡

Division of Allergy, Critical Care, and Respiratory Medicine, Department of Medicine, Duke University Medical Center, Durham, North Carolina 27710; †Department of Chemistry, Duke University, Durham, North Carolina 27710; and ‡Respiratory, Critical Care, and Occupational (Pulmonary) Medicine, Department of Internal Medicine, University of Utah, Salt Lake City, Utah 84134

Received July 19, 1993, and in revised form February 2, 1994

Surface functional groups on silicate dusts complex iron cations which can cycle through reduction and oxidation states to generate free radicals. These oxidants have a capacity to produce DNA strand breaks and mutations which are primary events in cancer induction. A differential in the capacity of fibrous silicates to produce carcinoma is recognized with the amphiboles demonstrating a greater biologic effect than the serpentine fiber chrysotile. We tested the hypothesis that the differences in genotoxicity of these fibrous silicates correspond to varying concentrations of iron complexed to the surface. Relative to chrysotile, the amphibole fibers complexed greater amounts of iron cations from both inorganic and *in vivo* sources. Increased concentrations of surface-complexed iron were associated with greater oxidant generation, measured as thiobarbituric acid-reactive products of deoxyribose, and more covalently closed, circular DNA strand scission. These results indicate that genotoxic effects of these fibers may correspond to their capacity to complex iron at the surface. © 1994 Academic Press, Inc.

Inhalation of fibrous silicates increases the incidence of lung neoplasms and mesothelioma. The mechanism of cancer induction is not known. Carcinogenicity is postulated to reflect parameters of particle geometry and the contingent capacity of the lung to clear the dust (1). Inability to move the longer, thinner fibers from the lung is proposed to result in their endocytosis, potential interaction with the mitotic apparatus of the cell, and chromosomal aberrations (2). An alternative hypothesis of genotoxicity and cancer induction suggests that oxidants generated by fibrous silicates are associated with DNA damage (3, 4). Acidic functional groups on the surface of mineral oxides have a capacity to complex transition metals, especially iron, which catalyze electron transport (5). Free radicals are generated during the oxidation of ferrous to ferric ions:

$$Fe^{2+} + H_2O_2 \rightleftharpoons Fe^{3+} + {}^{\cdot}OH + {}^{-}OH$$

$$Fe^{2+} + H_2O_2 \rightleftharpoons Fe(OH)^{2+}_2.$$

The products of the reaction between Fe^{2+} and H_2O_2 are debated, but both hydroxyl ($^{\cdot}OH$) and ferryl ($Fe(OH)^{2+}_2$) radicals can affect DNA strand breaks (6, 7). In addition, oxidants could possibly function to activate oncogenes or inactive anti-oncogenes (8, 9). A differential in the capacity of fibrous silicates to produce mesothelioma and carcinoma is recognized with the amphiboles, including amosite ($[Fe^{2+},Mg]_7[Si_8O_{22}][OH]_2$) and crocidolite ($Na_2[Fe^{2+}]_3[Fe^{3+}]_2[Si_8O_{22}][OH]_2$), demonstrating a biologic effect greater than that of the serpentine fiber chrysotile ($Mg_3[Si_2O_5][OH]_4$) (10, 11). We tested the hypothesis that the differences in genotoxicity of silicates correspond to varying concentrations of iron complexed to the fiber surface which can catalyze the generation of oxidants and therefore affect DNA damage.

MATERIALS AND METHODS

Materials. All materials were obtained from Sigma Co. (St. Louis, MO) unless specified. Buffers were treated with chelating resin (Chelex 10 g/500 ml) for 2 h with agitation to diminish available iron cations.

Characterization of silicates. The surface areas of amosite, crocidolite, and chrysotile (National Institute of Environmental Health Sciences,

[1] To whom correspondence should be addressed at Duke University Medical Center, Box 3177, Durham, NC 27710.

0003-9861/94 $6.00

Research Triangle Park, NC) were determined using the Brunauer–Emmett–Tell (BET)[1] nitrogen adsorption isotherm.

The functional group present in silicates with the greatest surface acidity constant is the *silanol* group (–SiOH), which is significantly deprotonated at physiologic values of pH and therefore will coordinate many available metal cations (12). Random parting and fracture of fibers during the collection and processing of the silicate should position structural components at the surface in proportion to quantities in the crystal lattice. Therefore, surface silanol density should parallel percentage SiO_2 within the crystal. Percentage SiO_2 of the silicates was quantified after fusion ($LiBO_2/LiB_4O_7$; 10:1, w/w) at 1000°C. The melt was quenched in a mix of H_2O_2, HNO_3, and tartaric acid. Silicon was measured in duplicate specimens using inductively coupled plasma spectroscopy (Perkin Elmer P2000). Surface silanol concentrations were determined in triplicate specimens after washing 0.500 g of the fiber twice with 50 ml of 2 N HCl for 30 min at room temperature. Dissolution of the dust during this time was measured by atomic absorption as release of silicon into the supernatant and was negligible for all three fibers. The dusts were centrifuged, washed in distilled water, and suspended in 0.01 N NaOH. This colloidal suspension was agitated for 1 h and centrifuged at 1200*g* for 10 min. Three drops of 1% phenolphthalein in isopropanol were added to the supernatant and this was titrated to a colorless endpoint with 0.010 M HCl and the volume of titrant compared with that required to neutralize the same volume of 0.01 N NaOH which had not been exposed to dust (13).

Surface concentrations of iron. Surface iron was measured by exposing 30.0 mg of amosite, crocidolite, and chrysotile to 0.3 M sodium citrate, 1 M sodium bicarbonate, and 100 mg dithionite. This colloidal suspension was agitated in a water bath at 70°C for 30 min, centrifuged at 1200*g* for 10 min, and the supernatant assayed for iron in triplicate specimens by a spectrophotometric method employing 1,10-phenanthroline.

Surface iron after intrapleural injection. To evaluate complexation of iron by fibrous silicates after introduction into a living system, Sprague–Dawley rats (Charles River Breeding Labs, Wilmington, MA) were intrapleurally injected with 30 mg of either amosite, crocidolite, or chrysotile (six rats/silicate) while under anesthesia with halothane (2–5%). Ninety-six hours later, rats were anesthetized and exsanguinated, the pleural cavity was lavaged with 10 ml saline, and the lungs were excised. Collected fluid and tissue were digested with 5.25% (w/v) NaOCl (50 ml/g tissue) and passed through filters with a pore size of 0.45 μm (Millipore, Bedford, MA). Accumulated dust was washed 10 times with water and surface iron was assayed in triplicate employing the citrate–bicarbonate–dithionite method.

Surface and total iron after saturation with ferric chloride. To simulate the *in vivo* effect of increasing surface iron and to examine any consequences this has on oxidant generation and DNA strand breakage, the surfaces of fibrous silicates were saturated with a ferric salt. Amosite, crocidolite, and chrysotile were exposed to 1 mM $FeCl_3$ and the suspensions agitated for 15 min. Solutions were used immediately after preparation. Approximately 1% of Fe^{3+} in the ferric chloride solution precipitated out as insoluble oxyhydroxides within 1 h and contamination of the silicates with these compounds is negligible. Suspensions were centrifuged, washed with distilled water 10 times, and the fibers were examined for surface iron in triplicate. Oxidant generation and cccDNA strand breakage by these silicates with increased surface concentrations of complexed iron were also measured.

Total iron in crocidolite was determined prior to and after exposure to 1 mM $FeCl_3$ for 15 min. Crocidolite 50 mg was digested in 3.6 M H_2SO_4 and 48% HF at 100°C for 30 min (open). This reaction was quenched with 10% boric acid and iron measured, after reduction with dithionite, in triplicate using a spectrophotometric method employing 1,10-phenanthroline.

Oxidant generation. Iron has a capacity to transfer electrons and generate oxidants (14). Such catalysis in the presence of 2-deoxy-D-ribose yields malondialdehyde-like products which can be measured as thiobarbituric (TBA) reactive products (15). The reaction mixture contained 1 mM deoxyribose, 1 mM H_2O_2, 1 mM ascorbate, and either 1 mg/ml silicate or 1 mg/ml silicate following exposure to $FeCl_3$. In an attempt to inhibit radical production, the hydroxyl radical scavenger dimethylthiourea (DMTU) and the iron chelator deferoxamine were added with final concentrations of 20 mM and 2.5 mM, respectively. For comparison with amphiboles containing iron coupled with oxygen within the structural lattice, iron oxides were similarly tested for a capacity to generate oxidants. FeO, Fe_2O_3, and Fe_3O_4 (1 mg/ml) were included in reaction mixtures with deoxyribose, H_2O_2, and ascorbate. The suspensions were incubated at 37°C for 1 h with agitation and then centrifuged at 1200*g* for 10 min. One milliliter of both 1.0% (w/v) TBA and 2.8% (w/v) trichloroacetic acid were added to 1.0 ml of supernatant, heated at 100°C for 10 min, cooled in ice, and the chromophore determined in triplicate specimens by its absorbance at 532 nm.

DNA strand breaks. Following exposure to oxidants, covalently closed, circular DNA (cccDNA) is converted to an open circular form (16). Ethidium bromide binds the latter intercalatively with a resultant increase in fluorescence intensity. A suspension of 2.5 μg negatively supercoiled PM2 bacteriophage cccDNA (Boehringer Mannheim, Indianapolis, IN), 1 mM H_2O_2, 250 μg fibrous silicate, or 250 μg fibrous silicate following exposure to $FeCl_3$, and 0.1 mM ascorbate was incubated for 1 h at room temperature and centrifuged at 10,000*g* for 10 s. In an attempt to inhibit DNA strand breakage, the hydroxyl radical scavenger DMTU and the iron chelator deferoxamine were added with final concentrations of 20 and 2.5 mM, respectively. FeO, Fe_2O_3, and Fe_3O_4 (250 μg) were similarly tested for a capacity to induce cccDNA breaks. Ethidium bromide (2.5 μg) was added to 250 μl of the supernatant. This was heated at 95°C for 4 min, cooled in a 25°C water bath, and the fluorescence measured with excitation at 525 nm and emission at 600 nm. Native PM2 cccDNA was defined to exhibit a relative fluorescence value of 0%. Calf thymic DNA served as a positive control (relative fluorescence of 100%). Measurements were made in replicates of five.

Statistics. Data are expressed as mean ± standard deviation. Analysis of variance was used to determine differences between multiple groups (17). When F ratios were significant, means were compared using Duncan's Multiple Range Test (18). Significance was assumed at $P < 0.05$.

RESULTS

The amphibole fibers amosite and crocidolite had lower surface areas, but a higher percentage SiO_2 relative to chrysotile (Table I). These values approximate reported values of SiO_2 for amosite, crocidolite, and chrysotile (19). The remainder of amosite and crocidolite includes iron (29.8 and 33.4%, respectively), sodium (0.0 and 4.9%, re-

TABLE I

Surface Area, Percentage SiO_2, and Surface Silanol Density of Fibrous Silicates

Silicate	Surface area (m^2/g)	Percentage SiO_2	Surface silanol density (groups/nm^2)
Amosite	2.3 ± 0.4	49.2 ± 0.5	7.6 ± 1.8
Crocidolite	8.7 ± 1.0	48.5 ± 0.3	4.7 ± 0.6
Chrysotile	28.8 ± 1.4	39.8 ± 0.9	1.8 ± 0.1

[1] Abbreviations used: BET, Brunauer–Emmett–Tell; TBA, thiobarbituric; DMTU, dimethylthiourea; cccDNA, covalently closed, circular DNA.

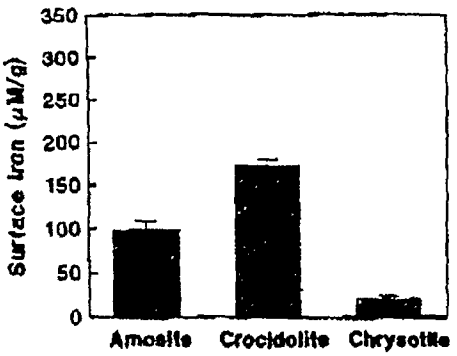

FIG. 1. Concentrations of iron complexed to the surface of fibrous silicates. There were significant differences among the three fibrous silicates. Crocidolite had the greatest concentration of surface-complexed iron while, despite the highest surface area, chrysotile had the least.

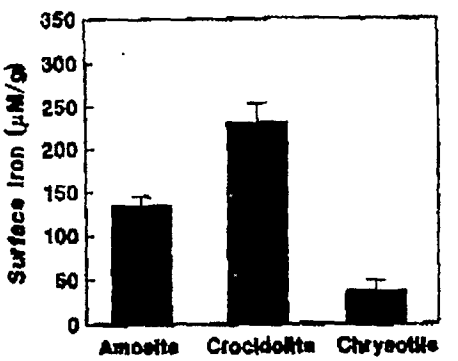

FIG. 2. Surface complexation of body sources of iron by silicate dusts. After introduction into an animal, fibers complexed further concentrations of iron. Significant differences were found among all three dusts, with crocidolite adsorbing the greatest concentrations of iron and chrysotile the least.

spectively), and magnesium (14.5 and 0.0%, respectively), while chrysotile has magnesium within its brucite layer (26.3%). Consistent with the measured percentage SiO_2, the concentration of surface silanol groups was higher in amosite and corcidolite relative to chrysotile (Table I).

Weathering in the inorganic environment of numerous primary minerals, including olivine, pyroxenes, biotite, magnetite, ilmenite, iron sulfides, and iron carbonates, makes Fe^{3+} and Fe^{2+} available to the silicates for complexation (20). Using the citrate–bicarbonate–dithionite assay, significant quantities of iron were found on all three dusts (Fig. 1). The concentrations of chelatable iron on both amphiboles were greater than that on chrysotile. These quantities may reflect some mobilization of lattice iron in addition to metal coordinated at the surface (21).

With *in vivo* exposures, fibers accrue iron and protein to produce ferruginous bodies. In addition, cells which phagocytose fibers demonstrate a rapid accumulation of iron (22). Both observations suggest that the surfaces of silicates are not saturated with the metal. Surface-complexed iron can be of importance in the induction of disease after silicate exposure only if the host cannot eliminate the coordinated metal. After intrapleural injection, the three fibrous silicates complexed *in vivo* sources of iron (Fig. 2). Again, the concentrations of surface iron were greater on the amphiboles compared to chrysotile.

To delineate the effect of increased surface complexed iron observed after *in vivo* exposure, amosite, crocidolite, and chrysotile were saturated with Fe^{3+}. Greater concentrations of Fe^{3+} were necessary to saturate the surfaces of amosite and crocidolite (Fig. 3). Amphiboles have higher concentrations of lattice iron than chrysotile and these differences in structural metal could theoretically account for variation in the associations of asbestos with oxidant generation, genotoxicity, and cancer. There was no difference in the total iron of crocidolite prior to (31.8±1.6%) and after (30.3±2.1%) saturation of the surface with $FeCl_3$.

Differences between the fibers in TBA-reactive products paralleled the concentrations of surface complexed iron (Fig. 4). DMTU and deferoxamine diminished TBA-reactive products so that the concentrations approached values found in mixtures without fibers (A_{532} = 0.064 ± 0.004). The absorbances observed for oxidized products in the presence of FeO, Fe_2O_3, and Fe_3O_4 did not differ significantly from control reaction mixtures with no fibers included.

Amphibole exposure also resulted in a higher frequency of cccDNA strand nicks than that observed with chrysotile exposure (Fig. 5). Similar to previous investigation (4), no increase in cccDNA strand breaks was observed on incubation with fibers in the absence of ascorbate. This suggests that concentrations of ferrous ion complexed to the fiber surfaces were small. DMTU and deferoxamine diminished DNA strand breaks to values not significantly different from cccDNA without fiber exposure. Compa-

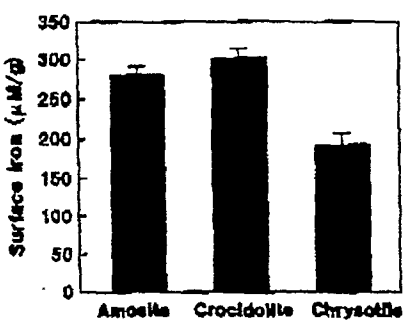

FIG. 3. Surface complexation of inorganic iron by fibrous silicates. The three fibers adsorbed Fe^{3+} from a solution of 1 mM ferric chloride over 15 min. Significant differences were demonstrated between the amphibole asbestos fibers and chrysotile. Differences between the amphibole fibers were not significant.

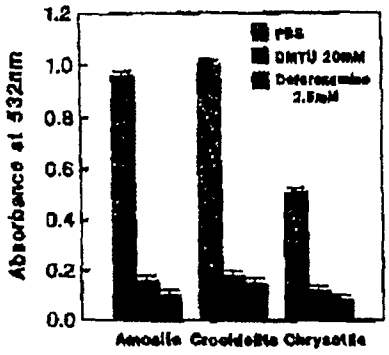

FIG. 4. Generation of oxidants by fibers measured as TBA-reactive products of deoxyribose. There were significant differences between the fibrous silicates with crocidolite and amosite having greater absorbance at 532 nm, reflecting higher concentrations of oxidative products of deoxyribose. Differences between the amphibole fibers were not significant. Both dimethylthiourea (DMTU) and deferoxamine significantly diminished oxidant products of deoxyribose after amosite, crocidolite, and chrysotile exposure.

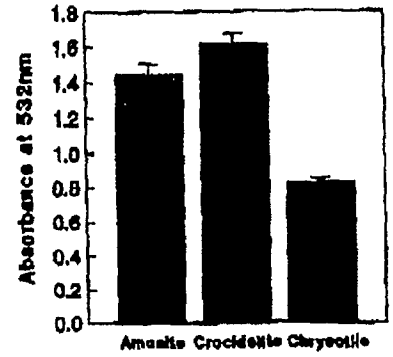

FIG. 6. Generation of oxidants by fibers after saturation of surfaces with iron. The amphibole fibers produced greater concentrations of oxidants, as reflected by the absorbance at 532 nm of TBA-reactive products of deoxyribose, after saturating the surfaces with Fe^{3+}. Differences between the amphibole fibers were not significant.

rable to oxidant generation, FeO, Fe_2O_3, and Fe_3O_4 did not significantly increase the frequency of cccDNA strand nicks above control values.

While saturation of the fiber surface had no effect on the total iron, TBA-reactive products of deoxyribose were greatly elevated again supporting a capacity of surface-complexed metal to catalyze electron transfer (Fig. 6). Disparities between the fibers in oxidant generation prior to and after saturation of the silicate surface with ferric chloride coincided with surface Fe^{3+} concentrations, suggesting that those dusts which accumulate iron after they are retained within an organism may have an increased capacity to produce free radicals. Finally, increased nicking of the cccDNA after saturation of the silicate surface with ferric chloride paralleled increments in both surface iron and oxidant generation (Fig. 7).

DISCUSSION

Major compositional differences between the asbestos fibers include (i) structural iron oxides and magnesium oxides within the lattices of the amphiboles and chrysotile, respectively, and (ii) a higher percentage of SiO_2 in amosite and crocidolite. Increasing the concentration of surface-complexed iron, while not altering the lattice metal content, greatly enhanced oxidant generation and cccDNA strand nicks. Although amosite and crocidolite have iron included in the crystal lattice, chrysotile has none in its ideal molecular formula. Isomorphic substitution of Fe^{3+} for Si^{4+} can account for the small quantity of iron in the lattice of this serpentine silicate. To mobilize this metal, there must be either dissolution of the silicate

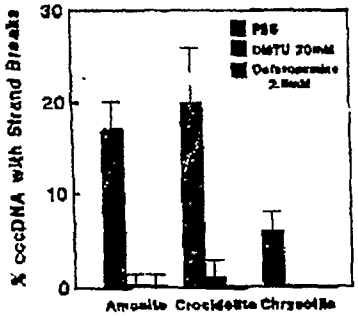

FIG. 5. DNA strand breaks resulting from the exposure of cccDNA to fibrous silicates. Incubations with amosite and crocidolite were associated with significantly more DNA strand breaks than chrysotile. Differences between the amphibole fibers were not significant. DMTU and deferoxamine both significantly diminished cccDNA strand breaks after amosite, crocidolite, and chrysotile exposure.

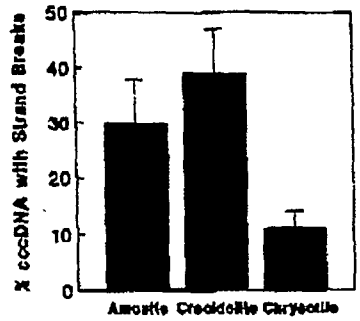

FIG. 7. DNA strand breaks resulting from the exposure of cccDNA to fibrous silicates after saturation of surfaces with iron. Incubations with amosite and crocidolite were associated with significantly more DNA strand breaks than chrysotile after saturation of their surfaces with iron. Differences between the amphiboles were not significant.

or an entry of a chelator into the lattice. Using [Si] as an indicator of dissolution of the silicate, no solubilization of the dust was noted. However, it is unlikely that a low-molecular-weight metal chelator could enter a crystal lattice which has interatomic distances of less than 1 Å, excise an iron cation bound within the lattice by strong crystalline forces, and exit the particle with the metal. Furthermore, iron oxides with the six coordination sites of the metal occupied, accordingly mimicking the state of the lattice iron in amosite and crocidolite, catalyzed neither electron transfer nor strand breakage. This evidence indicates that structural metal is unlikely to participate in free radical production in the *in vitro* systems employed. However, structural iron can catalyze heterogeneous electron transport. Structural oxidation of iron silicates occurs through an electron hopping mechanism. This can produce an increase of ferric cation in the lattice by reduction of surface Fe^{3+} (23). The surface iron can then be reoxidized by atmospheric O_2 (23). Certain compounds can also complex Fe^{2+} and accelerate mineral oxide dissolution (24–26). This can facilitate inner sphere electron transfer between structural and adsorbed iron states. Both of these mechanisms of electron transfer are ultimately dependent on the concentration of surface-complexed iron. The higher percentage of SiO_2 in amphiboles and the consequent greater density of surface silanol groups in these fibers result in an increased capacity to coordinate metal cations at the surface relative to chrysotile. Chrysotile would be expected to have the highest number of silanol groups per gram of dust of the three fibers examined (Table I). The low amounts of iron on the surface of chrysotile even after exposure to $FeCl_3$ (Figs. 1 and 3) indicate that the silanol densities (number of −SiOH per unit area) are more important than the absolute number of ligand groups in determining the amount of metal coordinated. The complexing groups must be close enough to each other on the mineral surface that a bi- or multidentate complex can be formed with the iron.

After introduction into a living organism, the three fibers complexed body sources of iron onto their surfaces. Disparities in the concentration of surface complexed iron between the amphiboles and chrysotile correspond with both oxidant generation and cccDNA scission, supporting a role for iron-catalyzed oxidant generation in the genotoxicity of fibers. DNA injury in $C3H10T_{1/2}$ cells after exposure to crocidolite was inhibited by iron chelators, possibly reflecting a dependence on the availability of incompletely coordinated iron (27). Products of oxidation reactions catalyzed by several other iron complexes are similarly mutagenic (28). Bleomycin, a glycopeptide employed as an anticancer drug, also coordinates iron and generates oxidants which cleave DNA (29). Such strand scission is inhibited by iron chelators (30). DNA damage after exposure of a microorganism to hydrogen peroxide was similarly dependent on both reducing equivalents and an availability of iron species (7). DNA scission by complexed iron predicts a carcinogenic potential in humans which is promoted by observations of osteosarcomas and hematopoietic neoplasms after intravenous injection of $^{59}FeCl_3$ (31). In further support of a role for this metal in genotoxocity, increased iron stores in humans elevate the risk of cancer in epidemiologic studies (32).

The endocytosis of the fiber is associated with oxidant generation and therefore should increase with the concentration of complexed iron and surface area (33, 34). Such endocytosis positions the silicate surface with the complexed transition metal in the proximity of DNA and iron may be transferred to the DNA, which also can coordinate this metal (35, 36). Subsequent oxidant generation could then result in strand breaks, genotoxicity, and cancer (37). A synergistic interaction between cigarette use and asbestos fibers in genotoxicity and induction of bronchogenic carcinoma is anticipated as a result of increased concentrations of lung iron available to be complexed by the fiber after smoking (38–40). The results of these investigations predict that, for a specified fibrous silicate, those particles which are longer and thinner, relative to short, thick fibers, will have greater values of both surface area and oxidant production with an increased probability of endocytosis and therefore the potential to induce DNA injury. Consequently the two postulates of cancer induction by fibrous silicates focusing on particle geometry and oxidant generation can be conciliated (1, 3, 4).

Based on our results, the carcinogenic potential of a fibrous silicate should be predicted by either surface concentrations of silanol groups, complexed [Fe^{3+}], or *in vitro* oxidant generation after saturation of the dust with an iron salt. The development of synthetic fibers with diminished carcinogenic potential will necessitate decreasing the number of surface functional groups with the capacity to complex iron and other transition metals which assume two stable valence states and can transfer electrons.

ACKNOWLEDGMENTS

We thank Dr. Mike Clark of Cyprus Minerals for assistance in surface area determinations and Dr. J. W. Stucki for guidance in surface iron measurements. This study was supported in part by grants from the National Institutes of Health (HL-02655) and the North Carolina Lung Association.

REFERENCES

1. Stanton, M. F., Layard, M., Tegeris, A., Miller, E., May, M., Morgan, E., and Smith, A. (1981) *J. Natl. Cancer Inst.* **67**, 965–975.
2. Hesterberg, T. W., and Barrett, J. C. (1985) *Carcinogenesis* **6**, 473–475.
3. Weinberg, E. D. (1980) *Lancet* **1**, 1399–1340.
4. Lund, L. G., and Aust, A. E. (1992) *Carcinogenesis* **13**, 637–642.
5. Schindler, P. W., and Stumm, W. (1987) in Aquatic Surface Chemistry. Chemical Processes at the Particle–Water Interface (Stumm, W., Ed.), pp. 83–110, Wiley, New York.

6. Hutchinson, F. (1985) *Progr. Nucleic Acid Res. Mol. Biol.* **32**, 115–154.
7. Imlay, J. A., and Linn, S. (1988) *Science* **240**, 1302–1309.
8. Crawford, D., Zbinden, I., Amstad, P., and Cerutti, P. (1988) *Oncogene* **3**, 27–32.
9. Heintz, N. H., Janssen, Y. M., and Mossman, B. T. (1991) *Proc. Natl. Acad. Sci. USA* **90**, 3299–3303.
10. Mossman, B. T., Bignon, J., Corn, M., Seaton, A., and Gee, J. B. L. (1990) *Science* **247**, 294–301.
11. McDonald, J. C., and McDonald, A. D. (1987) *in* Asbestos Related Malignancy (Antman, K., and Aisner, J., Eds.), pp. 57–78, Grune and Stratton, New York.
12. Schindler, P. W. (1981) *in* Adsorption of Inorganics at Solid–Liquid Interfaces (Anderson, M. A., and Rubin, A. J., Eds.), pp. 1–48, Ann Arbor Science, Ann Arbor, MI.
13. Arhland, S., Grenthe, I., and Noren, B. (1960) *Acta Chem. Scand.* **14**, 1059–1076.
14. Graf, E., Mahoney, J. R., Bryant, R. G., and Eaton, J. W. (1984) *J. Biol. Chem.* **259**, 3620–3624.
15. Halliwell, B., and Gutteridge, J. M. C. (1981) *FEBS Lett.* **128**, 347–352.
16. Lown, J. W. (1984) *Methods Enzymol.* **105**, 532–539.
17. Colton, T. (1974) Statistics in Medicine, Little, Brown, Boston.
18. Duncan, D. B. (1955) *Biometrics* **11**, 1–42.
19. Deer, W. A., Howie, R. A., and Zussman, A. (1966) An Introduction to the Rock Forming Minerals, Longman Scientific & Technical, New York.
20. Murad, E., and Fischer, W. R. (1988) *in* Iron in Soils and Clay Minerals (Stucki, J. W., Goodman, B. A., and Schwertmann, U., Eds.), pp. 1–18, Reidel, Boston.
21. Borggaard, O. K. (1988) *in* Iron in Soils and Clay Minerals (Stucki, J. W., Goodman, B. A., and Schwertmann, U., Eds.), pp. 83–98, Reidel, Boston.
22. Koerten, H. K., Brederoo, P., Ginsel, L. A., and Daems, W. T. (1966) *Eur. J. Cell. Biol.* **40**, 25–36.
23. Addison, C. C., Addison, W. W., Neal, G. H., and Sharp, J. H. (1962) *J. Chem. Soc.* 1468–1471.
24. Baumgartner, E., Blesa, M. A., Marinovich, H. A., and Marto, A. J. G. (1983) *Inorg. Chem.* **22**, 2224–2226.
25. Blesa, M. A., Borghi, E. B., Marto, A. J. G., and Regazzoni, A. E. (1984) *J. Colloid Interface Sci.* **98**, 295–300.
26. Borghi, E. B., Regazzoni, A. E., Marto, A. J. G., and Blesa, M. A. (1989) *J. Colloid Interface Sci.* **130**, 301–310.
27. Turver, C. J., and Brown, R. C. (1987) *Br. J. Cancer* **56**, 133–136.
28. Tullius, T. D., and Dombroski, B. A. (1985) *Science* **230**, 679–681.
29. Saunville, E. A., Peisach, J., and Horwitz, S. B. (1978) *Biochemistry* **17**, 2740–2746.
30. Byrnes, R. W., and Petering, D. H. (1991) *Biochem. Pharmacol.* **41**, 1241–1246.
31. Laistue, J. A., Burlington, H., Cronkite, E. P., and Reinecke, U. (1977) *Cancer Res.* **37**, 3545–3550.
32. Stevens, R. G., Jones, Y., Micozzi, M. S., and Taylor, P. R. (1988) *N. Engl. J. Med.* **319**, 1047–1052.
33. Ghio, A. J., Kennedy, T. P., Whorton, A. R., Crumbliss, A. L., Hatch, G. E., and Hoidal, J. R. (1992) *Am. J. Physiol.* **263**, L511–L516.
34. Hobson, J., Wright, J. L., and Churg, A. (1990) *FASEB J.* **4**, 3135–3139.
35. Barry, B. E., Wong, K. C., Brody, A. R., and Crapo, J. D. (1983) *Exp. Lung Res.* **5**, 1–22.
36. Andronikashvili, E. L., Morulishvili, L. M., Belokobilski, A. I., Kharabadze, N. E., Tevzieva, T. K., and Efremova, E. V. (1974) *Cancer Res.* **34**, 271–274.
37. Libbus, B. L., Illenye, S. A., and Craighead, J. E. (1989) *Cancer Res.* **49**, 5713–5718.
38. Selikoff, I. J., Hammond, E. C., and Churg, J. (1968) *J. Am. Med. Assoc.* **204**, 104–112.
39. Jackson, J. H., Schraufnagel, I. U., Hyslop, P. A., Voshell, K., Sauerheber, R., Weitzman, S. A., and Cochrane, C. G. (1987) *J. Clin. Invest.* **80**, 1090–1095.
40. Church, D. F., Burkey, T. J., and Pryor, W. A. (1990) *Methods Enzymol.* **186**(Part B), 665–669.

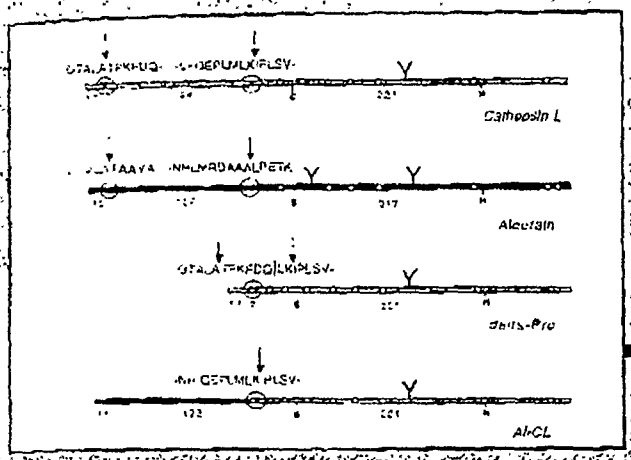

ARCHIVES OF Biochemistry and Biophysics

May 15, 1994

Academic Press
San Diego New York Boston London Sydney Tokyo Toronto